Front. Mater. Sci. China 2009, 3(1): 84–88
DOI 10.1007/s11706-009-0006-3

RESEARCH ARTICLE

Numerical simulation on bucking distortion of aluminum alloy thin-plate weldment

Jun LI (✉), Jian-guo YANG, Hai-long LI, De-jun YAN, Hong-yuan FANG

State Key Laboratory of Advanced Welding Production Technology, Harbin Institute of Technology, Harbin 150001, China

Abstract In this paper, the welding residual distortion of aluminum alloy thin plates is predicted using the elasticity-plasticity finite element method (FEM). The factors contributing to the welding buckling distortion of thin plates are studied by investigating the formation and evolution process of welding stresses. Results of experiments and numerical simulations show that the buckling appearance of thin-plate aluminum alloy weldments is asymmetrical in the welding length direction, and the maximum longitudinal deflection appears at the position a certain distance from the middle point of the side edge towards the arc-starting end. The angular deformation direction of thin-plate weldments is not fixed, and such case as the angular deformation value of the arc-starting end being higher than that of the arc-blowout end exists.

Keywords aluminum alloy, thin plate, welding, buckling distortion, numerical simulation

1 Introduction

As aluminum alloys are characterized with light weight and excellent processing properties, the welded structures of aluminum alloy thin-plates are widely used in aerospace industry, automotive industry, railway engineering, ship-building engineering, etc. [1]. However, due to the large linear expansion factor and the solidification shrinkage ratio, serious welding residual distortions have always been found in the welded structures made of aluminum alloys. As is known, when aluminum and its alloy materials cool from the liquid state to the solid state, there will be obvious volume shrinkage as large as about 6%. Welding deformation can seriously affect the dimensional accuracy of welded structures, often leading to the failure of products in meeting the requirements of design [2]. Therefore, the study on controlling residual stresses and distortion of aluminum alloy thin-plate weldments is always a significant subject in the welding engineering [3]. In this paper, the finite element analysis software Marc was used to numerically simulate the buckling distortion of aluminum alloy thin plates with a straight welding seam, based on which we analyzed the formation reasons and the mechanism of the welding distortion, in order to provide a theoretical reference to effectively control the residual distortion.

Received September 22, 2008; accepted October 18, 2008

E-mail: lijun20066002@sina.com.cn

2 Establishment of FEM

Figure 1 shows the finite element model of the workpiece, which is 270 mm in length, 130 mm in width and 2 mm in thickness, consisting of 25192 elements. In the area the welding heat source passes through, there are refined elements with the dimension of 1 mm×1 mm×1 mm. The material used here is aluminum alloy 2A12T4. Some material parameters under room temperature are set as follows: yield strength, 330 MPa; Young's modulus, 66.7 MPa; thermal conductivity, 119 W/(m·K); specific heat, 900 J/(kg·°C); thermal expansion coefficient, 2.28×10^{-5}/°C. These parameters vary with temperature, as shown in Figs. 2 and 3.

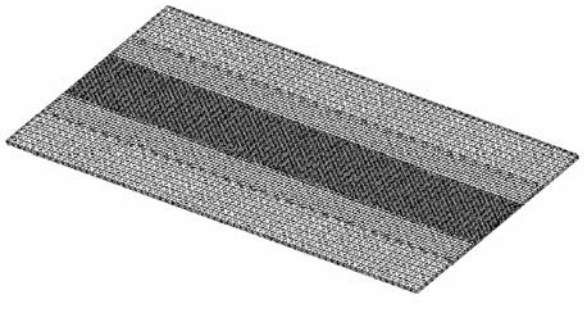

Fig. 1 Finite element model of workpiece

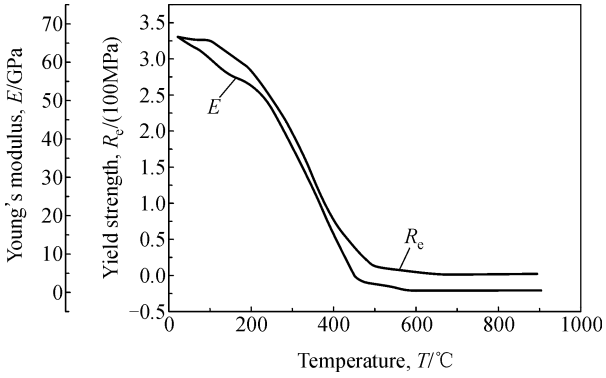

Fig. 2 Temperature dependency of yield strength and Young's modulus in case of 2A12T4 aluminum alloy

The welding method adopted is TIG. Table 1 gives the welding parameters used in the FEM (finite element method) analysis. The Double-Ellipsoid heat source model has been chosen for the calculation process.

To make the calculation model agree with actual welding conditions, three surfaces, which represent rigid welding fixtures, were taken to exert the restraint on the model (shown in Fig. 4), and were separated from the finite element model after welding. According to whether or not the faces of the finite element model have contact with those surfaces, different heat convection coefficients were set on the faces of the finite element model.

Table 1 Parameters of welding

Current I /A	Voltage U /V	Heat efficiency	Welding speed v /(mm·s^{-1})
120	12	0.5	4.75

3 Results and discussion

Figure 5 shows the simulation result of the welding residual distortion in the 2Al2T4 aluminum thin-plate weldment. The deformation display and the numerical distribution indicate that it is a typical saddle-shaped

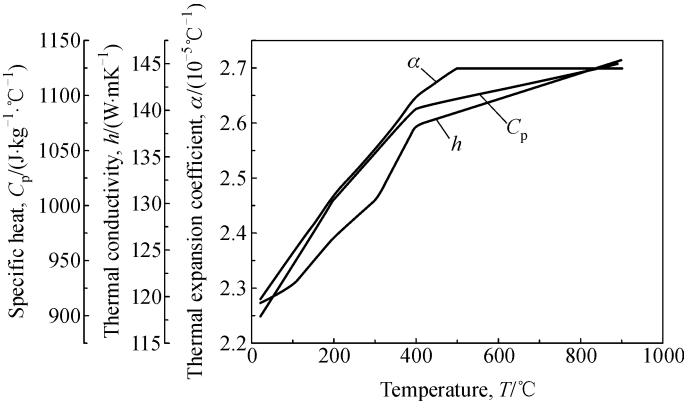

Fig. 3 Specific heat, thermal conductivity and thermal expansion coefficient temperature dependency in case of 2A12T4 aluminum alloy

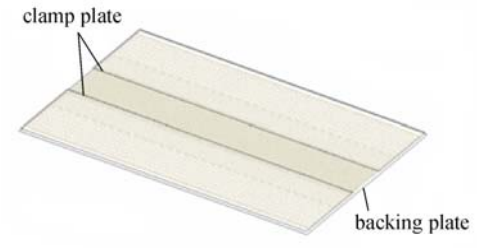

Fig. 4 Modeling of welding clamp

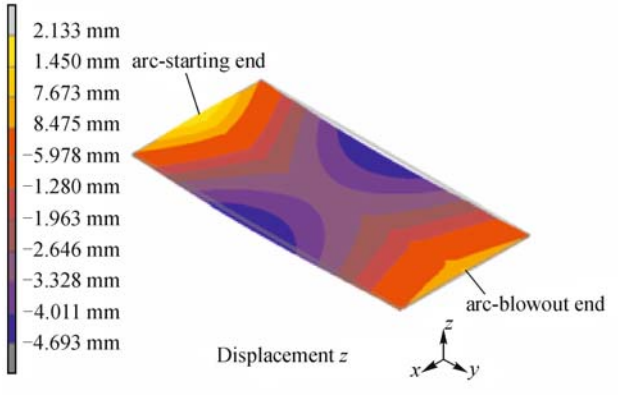

Fig. 5 Simulation result of residual distortion

distortion with downward deflection in the middle part of the plate. In any cross section of the weld, the downward angular deformation with symmetry on both sides referring to the weld line can be observed.

Figure 6 shows the defection curves of longitudinal sections at various distances from the weld seam center. It can be seen from this figure that the maximum longitudinal deflection, 4.69 mm, appears at the position on the side edge of the plate, 11.6 mm far from the arc-starting end of the weldment. Furthermore, the *D*-value of the deflection between two ends of the weld suggests that the angular deformation value of the arc-starting end is bigger than that of the arc-blowout end.

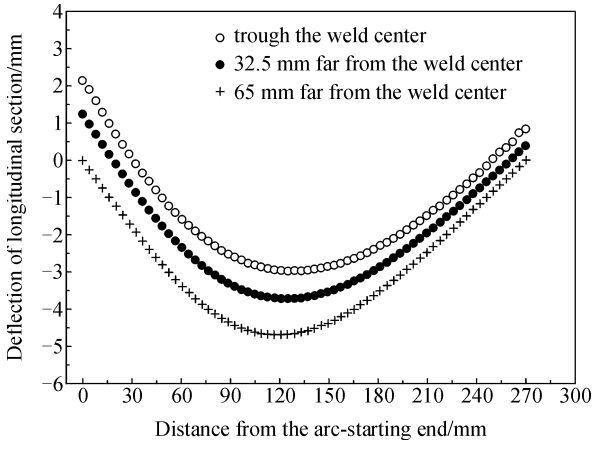

Fig. 6 Simulation results of deflection of longitudinal sections different distances from the welding line

In order to validate the simulation results, welding experiments were performed on thin plates with the same material and size as the model. The welding parameters were also the same as those of the model. Figure 7 shows a typical thin-plate welded piece using alternating argon tungsten-arc without the filler metal, and Fig. 8 shows the deflection measurement results of three longitudinal sections at different distances from the weld seam. It can be observed easily from such two figures that the deformation shape of the actual weldment greatly resembles that of the simulated weldment. The maximum longitudinal deflection, 5.78 mm, of the actual weldment also appears in the side edges of the plate, which is 12 mm far from the arc-starting end of the weldment. The measurement results reveal that the angular deformation of the arc-starting end is 3.1°, 1.1° more than that of the arc-blowout end.

Four nodes, named respectively as A, B, C and D, were taken in the cross section, 132 mm distant from the arc-starting end. Thereinto, node A lies in the weld center, while nodes B, C and D are, respectively, 9 mm, 36 mm and 61 mm far from the welding center line. Figure 9 shows the change curves of the longitudinal stress at nodes A, B, C and D with time.

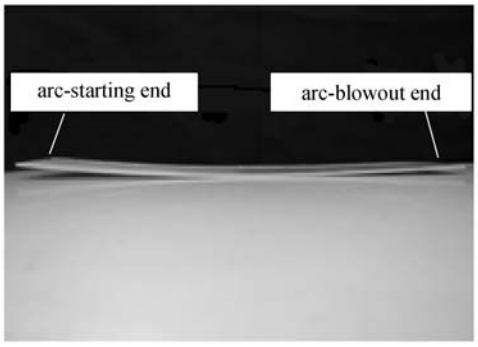

Fig. 7 Actual welded piece

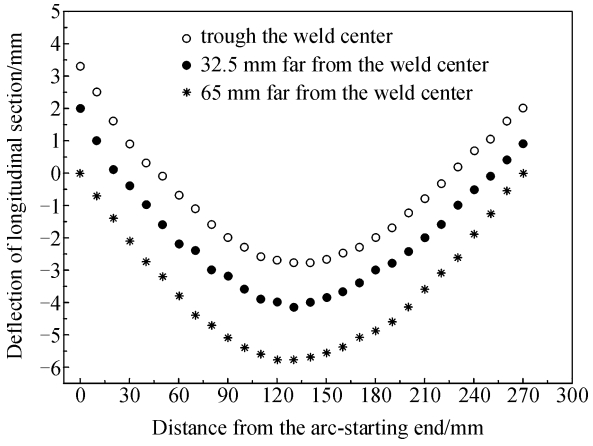

Fig. 8 Measurement results of deflection of longitudinal sections different distances from the welding line

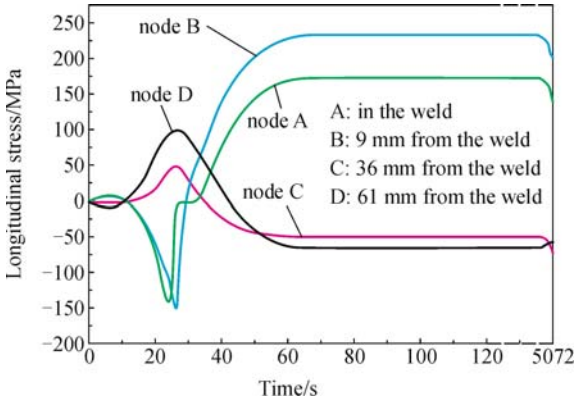

Fig. 9 Change of longitudinal stresses at nodes A, B, C and D with time

For node A, because of the rise of temperature, metals on both sides and in front of the weld pool expand, resulting in the compressive stress due to the restraint of surrounding metal at lower temperature. To balance it, the tensile stress appears on both sides of the compressive stress area. Under the drive of the tensile stress, the longitudinal stress state of node A shows the tensile stress. Because the distance

between node A and weld pool is far, the magnitude of the tensile stress of node A is low. With the approach of the heat source, the tensile stress increases at a slow speed, and thereafter decreases slowly till zero. With the further approach of the heat source, node A shows the compressive stress which continues to rise with temperature. When the distance between node A and the heat source center is about 19 mm, the temperature of node A is 98°C, and the compressive stress at node A reaches the maximum value of 141 MPa. After that, the compressive stress at node A begins to decline, and reaches zero quickly due to the sharp loss of mechanical properties of the weld metal. As the temperature of node A reaches the melting point, a platform appears just as shown in Fig. 9. Subsequently, node A goes into the cooling stage. In the cooling process of welding, the solidification shrinkage and the thermal contraction will occur, and the shrinkage magnitude of metal around the weld becomes less than that of the weld metal due to the relatively lower temperature. Thus, the weld metal is tensioned and the tensile stress appears at node A. The tensile stress at node A continuously increases with the drop of temperature until reaching a changeless value, here, 174 MPa. After the welded piece is free from the fixture, the tensile stress drops a little as a result of the redistribution of stresses in the whole welded piece.

Node B has similarities with node A in the evolution of the longitudinal stress. However, because the temperature of node B cannot reach the melting point, the evolution process of the longitudinal stress at node B has no horizontal line segment part like that of node A. Otherwise, the residual tensile stress of node B is higher than that of node A owing to the material properties of aluminum alloys. The evolution laws of the longitudinal stresses of nodes C and D are opposite to those of nodes A and B, which can be explained by that the generation and the change of stress in the area far from the weld seam is not caused directly by the welding heat source, but for the balancing of stress in the weld and its neighboring zone, which makes the sum of stress of whole weldment zero. The residual stresses at nodes C and D are compressive stresses.

Thus, after welding, the longitudinal residual stresses in and around the weld are tensile stresses and the longitudinal residual stress in the area far from the weld is the compressive stress. The buckling distortion will occur when the longitudinal residual compressive stress in the area far from the weld surpasses the critical compressive stress value of the thin-plate weldments [4]. Further, the difference in transverse shrinkage magnitude in plate thickness direction in the cooling stage may lead to the generation of angular deformation. The root reason of angular deformation is transverse shrinkage [5]. Generally speaking, because of the distinction in heat input and radiation conditions, the traverse shrinkage magnitude of the weld metal close to the façade of the welded piece is more than that of the weld metal close to the back face of the welded piece. Thus the angular deformation usually bends upwards. However, this rule does not hold true for thin-plate butt weldments, which are susceptible to the buckling deformation. This is due to the fact that the magnitude and the distribution of residual stresses in weldments vary with material properties, welding parameters, restraint conditions and so on. Moreover, the traversal shrinkage deformation and the longitudinal shrinkage deformation can influence each other. The buckling direction of the thin-plate weldments is not fixed, with one case bending upwards, another bending downwards, and other cases having two steady bucking directions. Thus, the direction of angular deformation occurring in thin-plate weldments is also hard to predict, and is determined by the minimum potential energy when the residual stress field is in steady state. It is traditionally considered that because of the effect of transverse shrinkage of an earlier welded seam on the later welded seam, the magnitude of angular deformation along the weld length direction is less at the beginning and increases gradually later [6], but the angular deformations of actual weldments in this study do not meet such regularity. The case as angular deformation value of the arc-starting end being higher than that of the arc-blowout end can be often observed.

As regards thin-plate weldments with longitudinal weld seams, the maximal longitudinal deflection often appears at a position a certain distance from the middle point of the side edge towards the arc-starting end. The reason for it is analyzed to be the difference in contraction strain magnitudes in the welding path. During the heating, the temperature gradient in the fore part of the weld is larger than that in the rear part of the weld, so the longitudinal shrinkage magnitude in the fore part of the weld is greater than that in the rear part of the weld. Figure 10 shows the distribution of longitudinal residual stresses along the welding line. It can be observed in this figure that the peak value of longitudinal residual stresses lean to the arc-

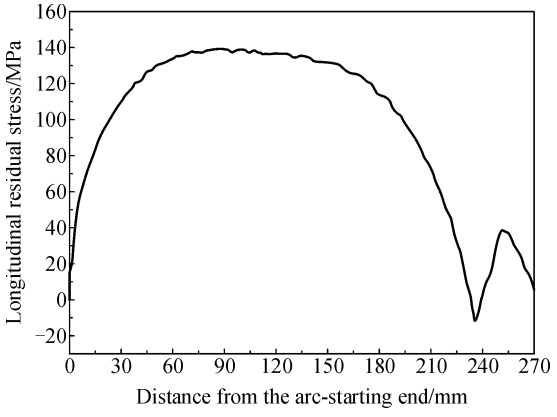

Fig. 10 Distribution of longitudinal residual stresses along the welding line

starting end. Because stress is the internal cause of the welding deformation, it is inevitable that the buckling deformation in the plate weldment with a straight weld seam is not symmetrical.

4 Conclusions

(I) There is serious buckling distortion in thin-plate aluminum alloy welded structures, which is asymmetrical in the weldment length direction and with the maximum longitudinal deflection appearing at a position a certain distance from the middle point of the side edge towards the arc-starting end.

(II) The residual tensile stress in and around the weld produced in the cooling stage of welding is the root reason for the buckling distortion of thin-plate weldments. The residual compressive stress in the area far from the weld is formed to balance the tensile stress in and around the weld. When the residual compressive stress exceeds the critical compressive stress of thin-plate weldments, buckling distortion will occur.

(III) The angular deformation of thin-plate weldments has no fixed form, and there is often higher angular deformation value at the arc-starting end than that at the arc-blowout end.

References

1. Zhang J Q, Zhang G D, Zhao H Y, et al. 3D-FEM numerical simulation of welding stress in thin aluminum alloy plate. Transactions of the China Welding Institution, 2007, 28(6): 5–9 (in Chinese)
2. Li Y J, Wang J. Welding and Application of Nonferrous Metal. Beijing: Chemical Industry Press, 2006, 29–30 (in Chinese)
3. Guan Q, Zhang C X, Guo D L. New technique for dynamically controlled low stress non-distortion welding. Transactions of the China Welding Institution, 1994, 15(1): 8–15 (in Chinese)
4. Guan Q. Efforts to eliminate welding buckling distortions — from passive measures to active in-process control. In: Proceeding of the 7th International Symposium of JWS: Today and Tomorrow in Science and Technology of Welding and Joining. Kobe, Japan, 2001
5. Fang H Y. Knowledge of Welded Construction. Beijing: China Machine Press, 2008, 94–95 (in Chinese)
6. Tian X T. Welded Construction. Beijing: China Machine Press, 1982, 29–32 (in Chinese)